environmental microbiology

Environmental Microbiology (2015) **17**(9), 3301–3313 doi:10.1111/1462-2920.12791

Hydrogen sulfide can inhibit and enhance oxygenic photosynthesis in a cyanobacterium from sulfidic springs

Judith M. Klatt,[1]* Sebastian Haas,[1] Pelin Yilmaz,[1] Dirk de Beer[1] and Lubos Polerecky[1,2]

[1]*Max-Planck-Institute for Marine Microbiology, Celsiusstrasse 1, Bremen 28359, Germany*

[2]*Department of Earth Sciences – Geochemistry, Faculty of Geosciences, Utrecht University, Budapestlaan 4, Utrecht 3584 CD, The Netherlands*

Summary

We used microsensors to investigate the combinatory effect of hydrogen sulfide (H_2S) and light on oxygenic photosynthesis in biofilms formed by a cyanobacterium from sulfidic springs. We found that photosynthesis was both positively and negatively affected by H_2S: (i) H_2S accelerated the recovery of photosynthesis after prolonged exposure to darkness and anoxia. We suggest that this is possibly due to regulatory effects of H_2S on photosystem I components and/or on the Calvin cycle. (ii) H_2S concentrations of up to 210 μM temporarily enhanced the photosynthetic rates at low irradiance. Modelling showed that this enhancement is plausibly based on changes in the light-harvesting efficiency. (iii) Above a certain light-dependent concentration threshold H_2S also acted as an inhibitor. Intriguingly, this inhibition was not instant but occurred only after a specific time interval that decreased with increasing light intensity. That photosynthesis is most sensitive to inhibition at high light intensities suggests that H_2S inactivates an intermediate of the oxygen evolving complex that accumulates with increasing light intensity. We discuss the implications of these three effects of H_2S in the context of cyanobacterial photosynthesis under conditions with diurnally fluctuating light and H_2S concentrations, such as those occurring in microbial mats and biofilms.

Received 24 September, 2014; revised 31 December, 2014; accepted 25 January, 2015. For correspondence. *E-mail jklatt@mpi-bremen.de; Tel. 0049 421 2028830; Fax 0049 421 2028690.

Introduction

Over the last centuries scientific interest in hydrogen sulfide (H_2S) was focused on its toxicity. This effect of H_2S is mainly based on the inhibition of cytochrome *c* oxidase, the enzyme catalyzing the last step of oxidative phosphorylation in respiration (Beauchamp *et al.*, 1984; Cooper and Brown, 2008). H_2S can therefore negatively affect a multiplicity of organisms including bacteria, animals (Beauchamp *et al.*, 1984; Dorman, 2002) and plants (Lamers *et al.*, 2013). In the last two decades, however, rising attention has been given to H_2S as a crucial metabolic regulator in higher organisms. In both animals and plants, H_2S serves as a gasotransmitter with diverse physiological functions (Hancock *et al.*, 2011; Wang, 2012). In plants, externally supplied H_2S was successfully tested as a growth-supporting agent, wherein the species-specific balance between the positive and toxic effects has to be considered (Lisjak *et al.*, 2013). The specific positive effects of both endogenously produced and externally provided H_2S include increased resistance against pathogens (Bloem *et al.*, 2004; Rausch and Wachter, 2005), improved freezing and heat tolerance (Stuiver *et al.*, 1992; Li *et al.*, 2012), protection against heavy metal toxicity (Zhang *et al.*, 2008; 2010) and drought resistance (Jin *et al.*, 2011). Besides increasing the stress tolerance, H_2S was also shown to be involved in the regulation of plant development (Rennenberg and Filner, 1983; Zhang *et al.*, 2008) and other complex processes such as stomatal closure (García-Mata and Lamattina, 2010; Lisjak *et al.*, 2010; Shen *et al.*, 2013).

In addition to these complex mechanisms, H_2S also impacts the basic constituents of oxygenic photosynthesis in plants. For instance, H_2S upregulates the expression of photosynthetic genes such as those coding for RuBisCO and ferredoxin (Chen *et al.*, 2011), promotes the activity of superoxide dismutase (Zhang *et al.*, 2009), induces an increase in the chlorophyll content (Zhang *et al.*, 2009; Chen *et al.*, 2011) and possibly affects photosystem stoichiometry (PSI:PSII ratio) (Dooley *et al.*, 2013). These components of photosynthesis had probably already evolved in the ancestor of all oxygenic phototrophs, most probably in a cyanobacterium (Mulkidjanian *et al.*, 2006).

This raises the question whether similar stimulatory functions of H_2S on photosynthesis can also be found in these bacterial oxygenic phototrophs. This would indicate that the positive regulatory effects represent evolutionarily old regulatory mechanisms thereby setting the basis for the development of further functions of H_2S in photosynthetic eukaryotes after the endosymbiotic event (McFadden, 2001).

Cyanobacterial oxygenic photosynthesis evolved in microbial mat-like structures (stromatolites) about 3.8–2.4 Ga ago (Buick, 2008). Possibly, these systems were characterized by intense sulfur cycling and abundant H_2S in the microenvironment of the early cyanobacteria (Nisbet and Fowler, 1999; Buick, 2008). Even after the first success of oxygenic photosynthesis in oxygenation of the atmosphere during the great oxygenation event, cyanobacteria still had to thrive in partially sulfidic oceans (Canfield, 1998; Johnston *et al*., 2009). Exposure of oxygenic phototrophs to H_2S therefore runs like a thread through the history of their evolution. Still, the oxygen evolving complex (OEC) of all contemporary cyanobacteria studied so far is inhibited to a species-specific degree by H_2S – even in species that are successful in sulfidic environments (Miller and Bebout, 2004). This suggests that the inhibitory effect of H_2S is evolutionarily deep rooted and that plausibly already the first OEC was vulnerable to H_2S toxicity. Consequently, cyanobacteria must have rapidly evolved strategies to cope with this toxicity and/or to even make use of H_2S. One strategy might have been the active depletion of H_2S by anoxygenic photosynthesis (Jørgensen *et al*., 1986). This capability to perform both oxygenic and anoxygenic photosynthesis is conserved in several specialized contemporary cyanobacterial species from sulfidic habitats (Cohen *et al*., 1975; 1986; Garcia-Pichel and Castenholz, 1990) (Klatt *et al*., 2015). The advantage of this strategy is the coupling of depletion of the toxic H_2S to energy conservation. In contrast, the strategies of obligate oxygenic phototrophic cyanobacteria that cannot photosynthetically deplete H_2S are comparatively poorly understood. So far, only Cohen and colleagues (1986) have shown for two cyanobacterial species that H_2S can act as a stimulator of photosynthetic rates under specific light conditions and H_2S concentrations. However, the parameter range, as well as the time frame over which this enhancement occurs, remains unclear.

Typical contemporary habitats of sulfide-adapted cyanobacteria are microbial mats and biofilms (Cohen *et al*., 1986; Jørgensen *et al*., 1986; Voorhies *et al*., 2012) that are regularly used as analogues for stromatolites (Seckbach and Oren, 2010). Due to the activity of their inhabitants and mass transfer limitations, these systems are generally characterized by steep vertical gradients in the concentrations of sulfide and oxygen (O_2), pH and light (Seckbach and Oren, 2010). Moreover, due to the diurnally fluctuating input of light energy, the conditions in these systems also change substantially on a temporal scale (Revsbech *et al*., 1983; Jørgensen *et al*., 1986). We hypothesized that all cyanobacteria that are competitive in such environments have special adaptations to H_2S and light dynamics, even if they are not able to actively deplete sulfide by anoxygenic photosynthesis. We therefore aimed to identify and elucidate possible adaptation mechanisms of obligate oxygenic phototrophic cyanobacteria to the fluctuating exposure to H_2S and light in such spatially heterogeneous and temporally dynamic systems. To fulfil this aim, we obtained a non-axenic mono-algal cyanobacterial culture from a thin microbial mat growing in a cold sulfidic spring and investigated its potential for anoxygenic photosynthesis and the inhibitory and stimulatory effects of H_2S on its oxygenic photosynthesis. The measurements were performed using microsensors in biofilms formed by the cyanobacterium with a set-up that allows creating artificial sulfide gradients across the biofilms (Fig. S1). We monitored the long-term effects of H_2S on photosynthesis and simulated diurnal light and H_2S fluctuations of natural microbial mats and biofilms.

Results

Studied strain

The studied cyanobacterium strain FS34 originates from a thin microbial mat sampled in the Frasassi sulfidic springs (Galdenzi *et al*., 2008). The cyanobacterium is filamentous (diameter of ~4 μm, length of up to ~100 μm; Fig. S2) and motile. The results of the tree reconstruction placed the sequence FS34 with other sequences of *Planktothrix* spp. (Fig. S2), and the sequence identity calculations returned values above 95%. Therefore, we propose that the isolate is a member of the genus *Planktothrix* and refer to it as *Planktothrix* str. FS34.

Planktothrix *str. FS34 does not perform sulfide-driven anoxygenic photosynthesis*

To determine whether *Planktothrix* str. FS34 can perform oxygenic and anoxygenic photosynthesis, the first experiments were conducted in a stirred batch reactor (Klatt *et al*. 2015). These experiments showed that *Planktothrix* str. FS34 can perform oxygenic photosynthesis in the presence of H_2S (Fig. S3). However, as total sulfide ($S_{tot} = [S^{2-}]+[HS^-]+[H_2S]$) was not consumed, we conclude that *Planktothrix* str. FS34 does not perform anoxygenic photosynthesis with sulfide as an electron donor within the studied range of irradiance (20–500 μmol photons m^{-2} s^{-1}).

During these batch reactor experiments, we observed the formation of biofilms and aggregates. Thus, the bulk measurements did not accurately reflect the conditions that the cyanobacteria were actually exposed to in their microenvironment, because O_2, pH and sulfide gradients typically develop within photosynthetically active biofilms (Wieland and Kühl, 2000). Although this does not invalidate the conclusion that they do not perform anoxygenic photosynthesis, further experiments were therefore performed in the biofilms with microsensors to accurately link the rates of photosynthesis to the local H_2S concentration.

Recovery of oxygenic photosynthesis after long-term exposure to darkness and anoxia

To study the effects of H_2S on the recovery of photosynthesis in *Planktothrix* str. FS34, we incubated biofilms of *Planktothrix* str. FS34 for ~10 h in the dark and anoxia and, after switching on the light, monitored the rates of gross photosynthesis (GP) together with the concentrations of O_2 and H_2S and pH inside the biofilm. After the first dark-anoxic incubation, which was done without H_2S, GP increased slowly after the onset of illumination, and the biofilm had to be illuminated for more than 6 h before GP reached an apparent steady state (Fig. 1A, triangles). After the next dark-anoxic incubation, which was done in a stable H_2S gradient across the biofilm achieved by the addition of sodium sulfide (Na_2S) stock solution to the reservoir of the flow cell below the biofilm (Fig. S1), switching on the light led to a remarkably faster recovery of GP than in the previous H_2S-free incubation (Fig. 1A, rectangles). The concentration of H_2S gradually decreased within the biofilm because of the equilibrium shift in the sulfide pool due to an increase in pH (Fig. 1B–D). When the H_2S concentration in the biofilm was still between 10 μM (surface) and 20 μM (1 mm depth), the GP rates at all depths reached a transient maximum that was between 1.5- and 2-fold higher than the apparent steady state level reached after ~6 h of incubation (Fig. 1A, rectangles). Intriguingly, the acceleration of the GP recovery as well as the level of the transient GP maximum were higher in deeper layers where H_2S concentrations were higher and light intensities plausibly lower (Fig. 1). When the same biofilm was again incubated in the absence of light, O_2 and H_2S, the recovery of GP after the light was switched on was again slow and gradual (data not shown). A long-term exposure of *Planktothrix* str. FS34 to H_2S in the dark and anoxia has therefore two effects on its photosynthesis: it accelerates the rate of photosynthesis recovery and induces a transiently higher rate than in a steady state reached several hours after the light becomes available.

Dynamics of the inhibition of photosynthesis by H_2S

To study the inhibitory effects of H_2S on photosynthesis in *Planktothrix* str. FS34, we incubated biofilms for ~6 h at different levels of incident irradiance and H_2S concentration and monitored O_2, H_2S, pH and the rate of GP in the uppermost layer of the biofilm. Before each measurement, we incubated the biofilm for 1–3 h in the dark under stable H_2S and O_2 gradients. In contrast to the results obtained after the long-term dark-anoxic incubations (see above), O_2 concentrations in the biofilm increased immediately when the light was switched on (data not shown). Additionally, H_2S concentrations concomitantly decreased due to a pH increase. When the H_2S concentration in the dark had been adjusted to 230 μM, the subsequent exposure to a low light (irradiance of 41 μmol photons m^{-2} s^{-1}) led to a rapid (within ~30 min) establishment of an apparent steady state (Fig. 2A). In this state, which we hereafter refer to as the 'active state', the cyanobacteria performed oxygenic photosynthesis at a constant rate while exposed to an H_2S concentration of 180 μM (Fig. 2A). However, this active state was stable only for ~3 h, after which GP rapidly decreased to zero (Fig. 2A). The cyanobacteria remained in this inactive state as long as H_2S was present. However, GP completely recovered within ~30 min after the H_2S was removed from the biofilm (data not shown). The inhibitory effect of H_2S was therefore reversible. In contrast to low light levels, a stable active state of photosynthesis in the presence of H_2S was not observed at higher light levels. For example, at irradiance of 130 μmol photons m^{-2} s^{-1}, the GP rate shortly increased after the onset of light, but then rapidly collapsed (Fig. 2B). At even higher light intensities, this peak of activity disappeared completely, and the cells were photosynthetically inactive immediately after exposure to light (data not shown). Thus, oxygenic photosynthesis in *Planktothrix* str. FS34 exhibits a biphasic pattern: it is not inhibited during a short-term exposure to H_2S, while a long-term H_2S exposure leads to an inhibition, which occurs faster at higher light intensities.

Temporary enhancement of oxygenic photosynthesis by H_2S at low light intensities

To study the stimulating effects of H_2S on photosynthesis in *Planktothrix* str. FS34, we measured the rates of GP in the uppermost layer of the biofilm as a function of irradiance (PI curves) and H_2S concentrations. Before each measurement, the biofilm was incubated in the dark with the O_2 concentration in the water column adjusted to ~20% air saturation and the H_2S concentration in the biofilm adjusted to a specific value by injecting the Na_2S stock solution into the bottom part of the flow cell. After the establishment of a stable H_2S gradient in the biofilm, the

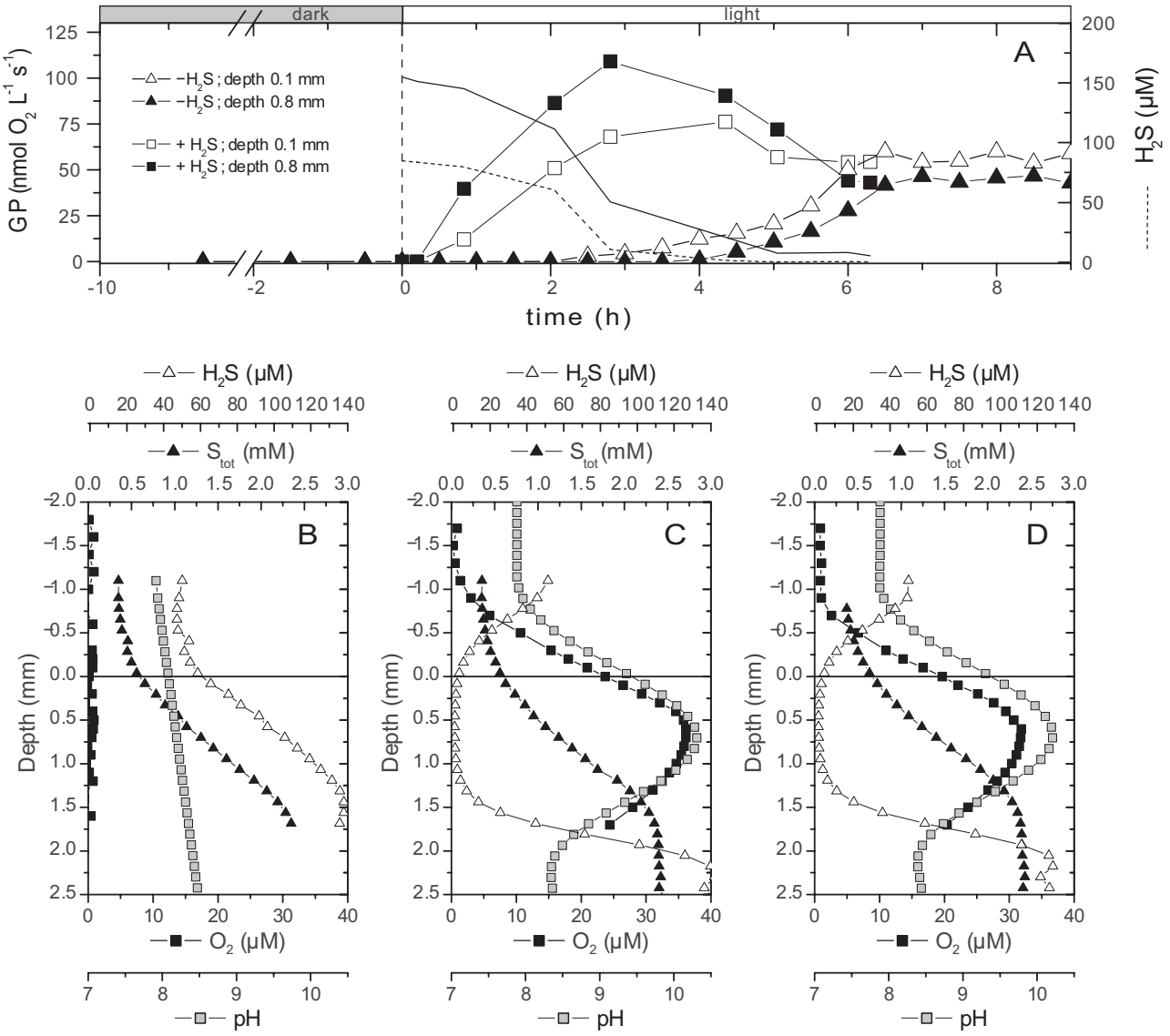

Fig. 1. Recovery of oxygenic photosynthesis in the *Planktothrix* str. FS34 biofilm after the long-term exposure to darkness and anoxia in the presence (+H_2S) and absence (–H_2S) of H_2S.
A. Volumetric rates of GP at two depths in the biofilm as a function of time, determined at incident irradiance of 69 µmol photons m^{-2} s^{-1}. The corresponding H_2S concentration measured at the same depths (dashed line: 0.1 mm, solid line: 0.8 mm) are also shown.
B–D. Depth profiles of O_2 and H_2S concentrations and pH measured in the biofilm at time points 0 h, 3 h and 6 h during the exposure to H_2S (+H_2S-treatment). S_{tot} concentrations were calculated from the local H_2S concentrations and pH.

light was switched on, which led to the dynamic increase and decrease of GP described above (see Fig. 2). When all measured parameters (GP, H_2S, pH) stabilized for more than 2 min, i.e. when a stable active state established, volumetric rates of GP and the H_2S concentration were recorded. Afterwards, the light was switched off to allow for an increase in the H_2S concentration in the measured point of the biofilm to the original value, and then GP measurements were repeated at higher light intensities. Subsequently, the concentration of H_2S was further increased by injection of Na_2S stock into the bottom part of the flow cell, and the entire procedure of GP measurements at different light intensities was repeated until partial PI curves at various H_2S concentrations were obtained.

In the absence of H_2S, the rate of GP exhibited a typical dependence on irradiance, increasing linearly at low light levels, reaching a maximum at some intermediate level and decreasing due to photoinhibition at high light levels (Fig. 3A). In contrast, the presence of sulfide induced

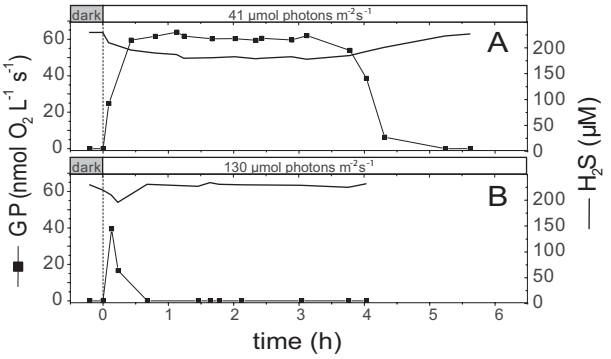

Fig. 2. Transition from the photosynthetically active state to an inactive state in *Planktothrix* str. FS34 biofilms. Gross photosynthesis rates were determined in the uppermost photosynthetically active layer of the biofilm at incident irradiances of 41 µmol photons m^{-2} s^{-1} (A) and 130 µmol photons m^{-2} s^{-1} (B). The corresponding H_2S concentrations were measured in parallel in the same layer of the biofilm.

complex patterns, wherein the interplay between both light intensity and H_2S concentration determined the photosynthetic rates (Fig. 3B). At H_2S concentrations below 150 µM, photosynthesis was enhanced at all light intensities, and no inhibition was observed within the time frame of the measurement. Interestingly, the increase of the GP rate with irradiance was quadratic in the irradiance range of 0–40 µmol photons m^{-2} s^{-1}, as opposed to an approximately linear increase in the absence of H_2S. Above 40 µmol photons m^{-2} s^{-1}, the GP rates gradually approached the values measured at zero H_2S concentration and continued to increase with a slope comparable to the slope at zero H_2S. However, there was a clear offset towards higher rates. At H_2S concentrations above 150 µM, the PI curve was characterized by a sharp decline above a certain threshold light intensity that decreased with increasing H_2S concentrations (Fig. 3B). This decline corresponded to the rapid collapse (within < 60 min) of the active state described above (see Fig. 2B). These clear patterns were only observed when plotted dependent on H_2S concentrations but not as a function of S_{tot} concentrations (data not shown).

Discussion

Oxygenic photosynthesis is the light-driven process of H_2O oxidation to O_2 coupled to the reduction of carbon dioxide (CO_2) to organic carbon. This coupling is facilitated by various redox reactions in the membrane (the electron transport chain) and in the cytosol during the Calvin cycle. Previous work has demonstrated that H_2S can affect a variety of these intermediate steps in plants and some cyanobacteria. For instance, H_2S inhibits the photosynthetic electron transport already during its first reaction when H_2O is split in the OEC (Miller and Bebout, 2004). The activity of photosystem I (PSI), which couples electron flow from PSII via the cytochrome b_6f complex to the last steps in the linear transport chain that serve $NADP^+$ reduction, appears to be upregulated (Dooley *et al.*, 2013). Also, H_2S increases the expression of the gene encoding for ferredoxin, one of the electron carriers between PSI and $NADP^+$ (Chen *et al.*, 2011). Even the activity of enzymes of the Calvin cycle is promoted by H_2S (Chen *et al.*, 2011).

Also our study demonstrates that the effects of H_2S can be multifaceted in a single organism. Specifically, H_2S appears to have three main effects on oxygenic photosynthesis in *Planktothrix* str. FS34: (i) It can accelerate the recovery of photosynthesis after exposure to darkness and anoxia, (ii) it can act as an inhibitor and, before inhibition occurs, (iii) it can temporarily enhance

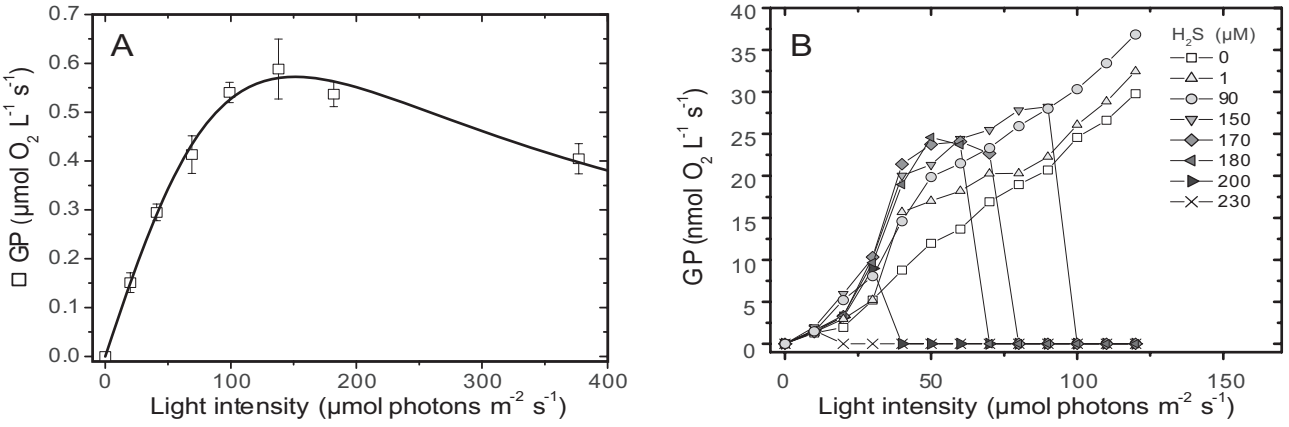

Fig. 3. Volumetric rates of GP as a function of incident irradiance (PI curves) measured in the uppermost layer of *Planktothrix* str. FS34 biofilms.
A. Complete PI curve in the absence of H_2S. The data points were fitted by the model of Eilers and Peeters (1988).
B. Partial PI curves measured at different H_2S concentrations in another biofilm sample.

photosynthesis during a time interval whose duration decreases with light intensity. We propose that these effects are caused by separate mechanisms that are discussed in the following.

Acceleration of the recovery of photosynthesis after exposure to darkness and anoxia

We observed a very slow recovery of the photosynthetic activity in *Planktothrix* str. FS34 after extended exposure to anoxia and darkness. Intriguingly, the recovery time was substantially shortened by H_2S (Fig. 1). A delay in the onset of photosynthesis after darkness and anoxia is a well-documented phenomenon in oxygenic phototrophs (Schreiber *et al*., 2002) and is explained by the fact that the Calvin cycle cannot be instantaneously activated. After long periods of darkness, ATP is depleted while NADPH is abundant. The latter cannot be oxidized to $NADP^+$ due to the limitation in ATP. Also the electron transport chain cannot become oxidized due to the limitation in the $NADP^+$ or other, external, electron acceptors such as O_2 (McDonald *et al*., 2011). In other words, without a terminal electron acceptor the non-cyclic oxygenic photosynthetic electron transport cannot be active. Consequently, photosynthetic ATP generation, which is crucial to generate the electron acceptor $NADP^+$ via the activity of RuBisCO, is inhibited. To overcome the problem of ATP limitation and over-reduction of the cellular components, oxygenic phototrophs generally use cyclic photophosphorylation in PSI (Schreiber *et al*., 2002). This process serves the generation of ATP in the absence of an electron acceptor for the non-cyclic oxygenic photosynthetic electron transport (Buchanan, 1991; Ghysels *et al*., 2013). H_2S might therefore increase the rate of cyclic photophosphorylation in PSI. This could, for instance, be accomplished by increasing the number of PSI reaction centres or associated pigments, as seen in *Zostera marina* seedlings (Dooley *et al*., 2013). Alternatively, it could also be achieved through an increased activity of ferredoxin, which is also involved in the cyclic electron transport, as observed in *Spinacia oleracea* seedlings (Chen *et al*., 2011).

However, because in the absence of H_2S the recovery time of photosynthesis after darkness and anoxia was extraordinarily long (up to 6 h, compared with minutes measured by Ghysels *et al*., 2013 or Schreiber *et al*., 2002), and the recovery was also delayed after prolonged darkness under aerobic conditions (up to 4 h, data not shown), it is more likely that H_2S has yet another crucial regulatory role. Enzymes involved in the Calvin cycle are generally activated indirectly by light. The mechanism behind this activation is the reduction of disulfide-bonds, which increases the catalytic capability of the respective enzyme. The reductant needed for this reaction is thioredoxin, which in turn receives electrons from ferredoxin at a light-dependent rate (Schürmann and Buchanan, 2008; Michelet *et al*., 2013). Therefore, we hypothesize that the function of H_2S in *Planktothrix* str. FS34 is similar to that of thioredoxin, i.e. it directly activates enzymes involved in the carbon fixation pathway by disulfide bond reduction. Further research is required to directly identify the mechanisms involved in the acceleration of the recovery of photosynthesis in *Planktothrix* str. FS34 after prolonged darkness.

Light-dependent inhibition of photosystem II activity by H_2S

We found that H_2S enhances photosynthesis in *Planktothrix* str. FS34 temporarily, i.e. during an active state. This active state can last for several hours at low light intensities but is substantially shortened or even disappears at higher light intensities (Fig. 2). The conspicuous light dependency of the inhibition in *Planktothrix* str. FS34 suggests that H_2S binds to an intermediate that is formed at a rate that is determined by the light intensity. We propose that this intermediate is generated during the light-driven water oxidation process in the OEC, because H_2S has been shown to inhibit PSII activity at its donor site (Miller and Bebout, 2004). We have incorporated this concept into a basic model of the electron transport processes in PSII (Fig. 4). Importantly, in our model, the reactions that actually convert the light energy into chemical energy, i.e. the excitation of the catalytic Chl *a* dimer in PSII (k_{E1}), the reduction of the primary electron acceptor Q_A (k_Q) and the generation of the intermediate in the OEC (k_C), are not directly affected by H_2S. They only indirectly depend on H_2S through an inactivation of an intermediate formed in the OEC. Because our data do not allow us to identify this intermediate, we refer to it generally as OEC_{ox}. Nevertheless, based on the present knowledge, this intermediate could be anything formed at the donor site of the catalytic Chl *a* – starting from the oxidized catalytic tyrosine residue that mediates electron transport between the reduced manganese centre of OEC to the oxidized P680 to any intermediate state formed in the S-cycle of OEC described in (Jablonsky and Lazar, 2008).

Numerical implementation of this model based on the rate laws described in Table 1 indeed enabled us to simulate the biphasic pattern of photosynthetic O_2 production observed in *Planktothrix* str. FS34 at low light intensities and the fast establishment of the inactive state at high light intensities (compare Fig. 2 with Fig. 5A and C). Specifically, the long-term stable active state at low light intensities occurs because the OEC is only slowly removed from the reactive pool through binding to H_2S (compare the evolution of OEC and OEC_{ox}:H_2S in Fig. 5B). This

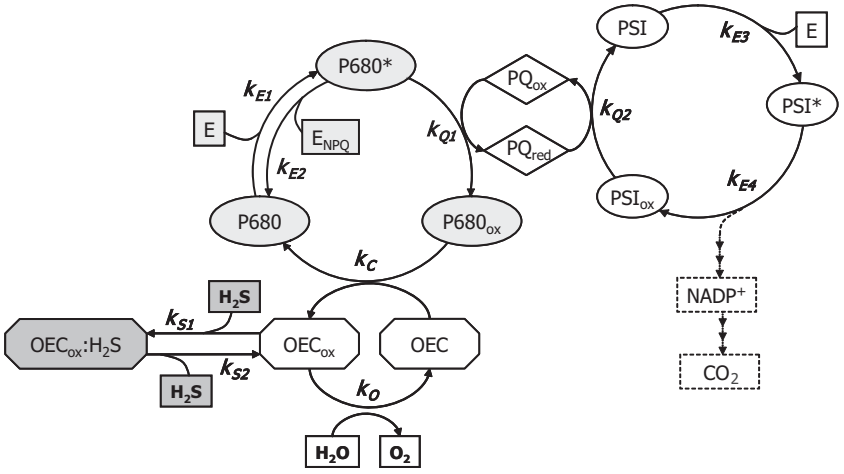

Fig. 4. Proposed model for the kinetic control of the reactions in the photosystem II of *Planktothrix* str. FS34 by H_2S. E is the photon flux; P680 and P680* is the Chl *a* dimer in the ground and excited state respectively; $P680_{ox}$ is the oxidized form of the Chl *a* dimer that receives electrons from the oxygen evolving complex (OEC). OEC_{ox} is the intermediate formed during H_2O oxidation that is inhibited by H_2S. OEC_{ox}:H_2S is the bound (and thus inhibited) form of this intermediate; PSI is the reaction centre of PSI in the ground state; PSI* is the excited catalytic Chl *a* in the PSI reaction centre; PSI_{ox} is the oxidized form of the PSI reaction centre that can receive electrons from reduced plastoquinone (PQ_{red}). Definitions of the process rates (k_i) are given in Table 1. Model implementation was done in R (www.cran.r-project.org) using the deSolve package (Soetaert *et al.*, 2010).

makes it still available for the interaction with the oxidized catalytic Chl *a* dimer in PSII ($P680_{ox}$), the generation rate of which is not directly affected by H_2S and continues dependent on the light intensity. Only upon inhibition of the complete OEC pool by H_2S does the photosynthetic rate rapidly decrease to zero. In contrast, a stable active state does not occur at high light intensities because the intermediate (OEC_{ox}) is generated at a higher rate, which leads to a more rapid accumulation of OEC_{ox}:H_2S and consequently to a faster depletion of OEC available for the oxidation by $P680_{ox}$ (Fig. 5D). We therefore conclude that the likely mechanism of the inhibition of oxygenic photosynthesis in *Planktothrix* str. FS34 is based on binding of H_2S to an oxidized intermediate of the oxygen evolving complex whose formation is driven by light.

Enhancement of the energy conservation efficiency in PSII and PSI by H_2S

Our data showed that oxygenic photosynthesis in *Planktothrix* str. FS34 is enhanced by H_2S at low light intensities (Figs. 1A and 3B). Intriguingly, H_2S appears to additionally transform the normally linear increase of photosynthesis with irradiance into a quadratic one (Fig. 3B). The initial slope of the PI curve is mainly determined by the energy conversion efficiency of PSII, while the decrease of the slope at higher light intensities and the resulting saturation of photosynthesis (Fig. 3A) are determined by the rate limiting steps downstream of PSII, which can either be plastoquinone diffusion time or carbon fixation rate in the Calvin cycle (Sukenik *et al.*, 1987; Cardol *et al.*, 2011). In *S. oleracea* seedlings, H_2S

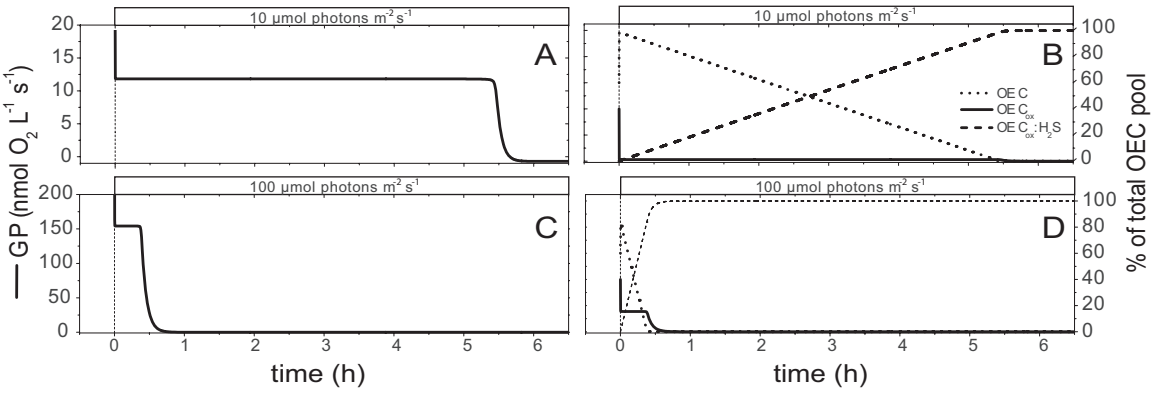

Fig. 5. Simulation of the transition from an active state to an inactive state in *Planktothrix* str. FS34. Shown are temporal dynamics of the volumetric rates of GP at low (A) and high (C) irradiance together with the corresponding partitioning of the OEC pool (B and D). In both cases, H_2S concentration of 200 µM was used. Note that the area under the two curves in (A) and (C), i.e. the total amount of O_2 produced, is the same. Thus, at a certain H_2S concentration a fixed amount of O_2 can be produced before complete inhibition occurs and only the time that it takes to generate this specific amount depends on light. In our model, this total amount of O_2 produced is defined by the ratio between the rates k_O and k_{S1} (k_O:$k_{S1} = \varepsilon/(\kappa\,[H_2S])$; Table 1).

Table 1. Definition of the rate laws governing the redox reactions shown in Fig. 4, and values of the constants used for the simulations in Figs. 5 and 6.

Expression[a]	Description	Constants[b]
$k_{E1} = \alpha$ E [P680] $\alpha = \alpha_0 + \eta$ E ([H_2S]/K_S + [H_2S])	The rate of generation of an excited catalytic Chl *a* dimer (P680*) in PSII. It depends on irradiance (E in μmol photons m^{-2} s^{-1}), the availability of the ground state Chl *a* ([P680] in nmol L^{-1}) and the absorbance cross-section factor α that describes the efficiency of conversion of the externally available photon flux into a volumetric rate of pigment excitation. The absorbance cross-section is assumed to increase with the H_2S concentration and irradiance.	$\alpha_0 = 1 \times 10^{-3}$ m^2 μmol^{-1} $\eta = 30 \times 10^{-6}$ m^4 s μmol^{-2} $K_S = 2$ μmol L^{-1}
$k_{E2} = \beta$ [P680*]	The rate of reformation of the ground state P680 from the excited state P680*. This reformation yields fluorescence and heat. Together with α, the parameter β determines the relation between the external photon flux and the potential electron transport rate.	$\beta = 1 \times 10^{-3}$ s^{-1}
$k_{Q1} = \gamma$[P680*]$\frac{[PQ_{ox}]}{K_g + [PQ_{ox}]}$	The rate of P680* oxidation coupled to the reduction of oxidized plastoquinone (PQ_{ox}). This process results in the formation of a highly reactive oxidized Chl *a* dimer ($P680_{ox}$).	$\gamma = 1$ s^{-1} $K_g = 50$ nmol L^{-1}
$k_{Q2} = \rho[PSI_{ox}]\frac{[PQ_{red}]}{K_r + [PQ_{red}]}$	The rate of reduced plastoquinone (PQ_{red}) oxidation coupled to the reduction of oxidized photosystem I (PSI_{ox}). This rate controls the availability of PQ_{ox} for the reduction by PSII and PSI in the ground state.	$\rho = 100$ s^{-1} $K_r = 5$ μmol L^{-1}
$k_C = \delta$ [$P680_{ox}$] [OEC]	The rate of generation of an intermediate in the oxygen evolving complex (OEC_{ox}), driven by $P680_{ox}$.	$\delta = 0.1$ L nmol^{-1} s^{-1}
$k_O = \varepsilon$ [OEC_{ox}]	The rate of H_2O oxidation to O_2 coupled to the reduction of OEC_{ox}. Division of k_O in nmol electrons L^{-1} s^{-1} by 4 gives the rate of oxygenic photosynthesis in nmol O_2 L^{-1} s^{-1}.	$\varepsilon = 1$ s^{-1}
$k_{S1} = \kappa$ [OEC_{ox}] [H_2S]	The rate of binding of H_2S to OEC_{ox}. This binding leads to the formation of OEC_{ox}:H_2S.	$\kappa = 20 \times 10^{-6}$ L μmol^{-1} s^{-1}
$k_{S2} = \sigma$ [OEC_{ox}:H_2S]	The rate of the reverse reaction that results in the release of OEC_{ox} from OEC_{ox}:H_2S.	$\sigma = 0.2 \times 10^{-6}$ s^{-1}
$k_{E3} = \theta$ E [PSI] $\theta = \theta_0 + \zeta\frac{[H_2S]}{K_H + [H_2S]}$	The rate of generation of an excited reaction centre in PSI. It depends on irradiance (E), the availability of the ground state PSI and the absorbance cross-section factor θ. In contrast to factor α, factor θ is assumed to increase only with the H_2S concentration but not with irradiance.	$\theta_0 = 1 \times 10^{-3}$ m^2 μmol^{-1} $\zeta = 2 \times 10^{-6}$ m^2 μmol^{-1} $K_H = 500$ μmol L^{-1}
$k_{E4} = \nu\frac{[PSI^*]}{K_E + [PSI^*]}$	The rate of photosystem I (PSI*) oxidation. PSI* oxidation is coupled to $NADP^+$ reduction and finally to CO_2 fixation in the Calvin cycle. Thus, we implemented the rate limitation in the Calvin cycle indirectly as a limitation of the PSI oxidation rate, which is given by the maximum rate ν.	$\nu = 900$ nmol L^{-1} s^{-1} $K_E = 4$ μmol L^{-1}

a. Rates are in nmol L^{-1} s^{-1}, where L refers to the volume of the biofilm.
b. The values correspond to the assumed concentrations of 1000 nmol L^{-1} for the total P680 pool (P680 + P680* + $P680_{ox}$), the total OEC pool (OEC + OEC_{ox} + OEC_{ox}:H_2S) and the total PQ pool (PQ_{ox} + PQ_{red}), and of 1500 nmol L^{-1} for the total PSI pool (PSI + PSI* + PSI_{ox}) in the biofilm.

increased the maximal photosynthetic rate but did not affect the initial slope of the PI curve (Chen *et al.*, 2011). This increase was accompanied by increased activity of RuBisCO and other photosynthetic components mediating the electron transfer between PSI and CO_2 (Chen *et al.*, 2011). Also in *Planktothrix* str. FS34, H_2S appears to affect PSI-associated electron transport, which accelerates recovery of photosynthetic rates after exposure to darkness (see above). The enhancement of the rates, however, cannot exclusively be based on this effect of H_2S. This is because the enhancement in *Planktothrix* str. FS34 occurred already in the range where the PI curve is normally linear and not in the range where light saturation occurs. Thus, the effect of H_2S cannot be limited only to the acceleration of electron transport downstream of PSII. We propose that H_2S also has an effect on the energy conversion efficiency in PSII.

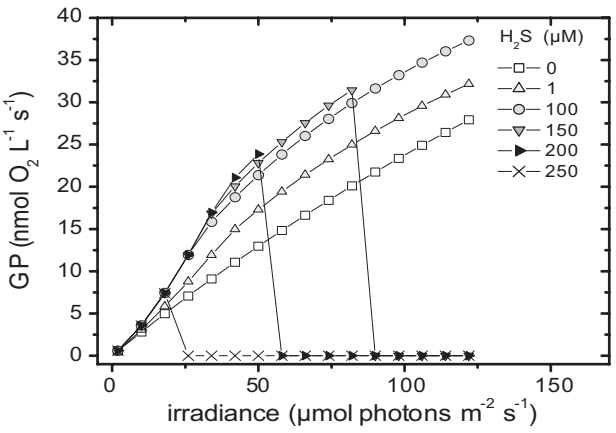

Fig. 6. Simulation of the PI curves in *Planktothrix* str. FS34 at different H_2S concentrations. The rates of GP are non-zero only if the active state was stable for more than 60 min.

Energy conservation efficiency can be increased by increasing the rate of excitation of the catalytic Chl *a* dimer, P680 (k_{E1} in Fig. 4), or by decreasing the rate of excitation energy loss into heat and fluorescence (k_{E2}). The rate k_{E1} can either be increased by increasing the pool of P680, i.e. the number of photosystems, or by increasing the absorption cross-section of PSII-associated pigments (factor α in Table 1). In our model, we assumed the latter. Specifically, we used the Michaelis–Menten kinetics with a low half-saturation constant (~2 μM) in combination with a linear function to describe the increase in the absorbance cross-section with H_2S and light respectively. Although we presently lack a mechanistic explanation for this increase, the most probable mechanism is a light-driven chemical transformation in PSII that leads to conformational changes and eventually to an increase in the absorbance cross-section. This would be consistent with the fact that the increase in photosynthesis is rapidly achieved (Fig. 2).

Assuming that only PSII activity is enhanced (k_{E1} in Fig. 4), rate limitation in PSI (k_{E3} in Fig. 4) is expected when k_{E1} approaches a certain threshold. This is because the electron transport components between PSII and PSI, e.g. plastoquinone (PQ), would become rapidly fully reduced and could not receive electrons from PSII anymore, which would slow down the complete electron transport process. The 'bump' on the PI curve at low irradiances indeed suggests that rate limitation in PSI plays a role above an H_2S-dependent light threshold. However, our data show that after this 'bump', the rates of photosynthesis are higher than those measured in the absence of H_2S. This implies that the potential PSI-associated electron transport rates must also increase in the presence of H_2S. A possible mechanism could be an increase in the maximum rate of CO_2 fixation in the Calvin cycle. However, since this positive effect on the Calvin cycle would mainly increase the slope of the PI curve above the 'bump', which would be inconsistent with our data, we deem this mechanism as unlikely. Another mechanism could be an increase in the absorbance cross-section in PSI (parameter θ in Table 1), plausibly due to the redistribution of excitation energy between the photosystems [state transition (Allen *et al.*, 1989)] or an increase of the number of PSIs in the thylakoid membrane. We implemented this by assuming that the parameter θ increases with H_2S according to the Michaelis–Menten kinetics but is light independent.

Numerical implementation of these mechanisms and empirically derived rate laws gave a reasonably good agreement between the experimentally determined (Fig. 3) and modelled (Fig. 6) PI curves. Therefore, we conclude that the stimulation of photosynthetic rates in *Planktothrix* str. FS34 by H_2S is likely based on (i) a rapidly saturated increase of the absorbance cross-section in PSII and (ii) a simultaneous, but less pronounced, increase of the light harvesting capabilities in PSI.

Implications for the ecophysiology of Planktothrix str. FS34

In microbial mats and biofilms, anoxygenic photosynthesis and aerobic sulfide oxidation (driven by photosynthetically produced O_2) are often responsible for the depletion of sulfide in the photic zone (Jørgensen *et al.*, 1986). These processes are, however, restricted to the times of daylight. During night, biotic and abiotic sulfide removal is limited by the supply of oxidant (e.g. O_2, NO_3^-) from the overlying water column, and consequently, sulfide concentrations in the photic zone generally increase (Jørgensen *et al.*, 1986). Our measurements reveal that during early mornings, such high H_2S concentrations, are not necessarily disadvantageous for obligate oxygenic phototrophic cyanobacteria such as *Planktothrix* str. FS34. Specifically, H_2S is even crucial to shorten the recovery time of photosynthesis after darkness during night and, especially under low light intensities, H_2S can temporarily increase the photosynthetic rate.

However, our data indicate that the niche of *Planktothrix* str. FS34 within sulfidic environments is rather narrow, as their activity strongly depends on defined temporal dynamics of H_2S and light, and their interplay. Specifically, the H_2S concentrations must be < 230 μM, otherwise, inhibition would occur instantaneously also at low light intensities, whereas at about 180 μM H_2S concentration and 40 μmol photons m^{-2} s^{-1}, photosynthesis is stable at an enhanced rate for more than 3.5 h. If comparable conditions occur in the microenvironment of *Planktothrix* str. FS34 during the early morning, it will rapidly recover from previous dark anoxic conditions and perform photosynthesis at an enhanced rate. Its oxygenic photosynthesis will then indirectly modulate the local H_2S concentration, even though it does not perform anoxygenic photosynthesis. Namely, the CO_2 fixation driven by oxygenic photosynthesis will lead to an increase in pH and thereby a decrease in H_2S in its microenvironment. Additionally, the H_2S levels will also decrease due to the uptake of sulfide by anoxygenic phototrophs and chemotrophic sulfide oxidizers. This means that the inactivation by H_2S (Fig. 2) will not occur in natural biofilms, as the sulfide species H_2S is quickly removed due to the strong photosynthesis-driven pH increase, similarly to the dynamics in Fig. 1. But even without efficient H_2S removal, it is expected that *Planktothrix* str. FS34 can remain in an active state for a complete day, given that the light intensity is very low. Also, *Planktothrix* str. FS34 is able to migrate inside a biofilm or a microbial mat, and

thus these cyanobacteria can plausibly escape from disadvantageous microenvironmental conditions. For instance, at 190 μM H_2S and 130 μmol photons, m^{-2} s^{-1} photosynthesis is completely inhibited after ~30 min. Migrating either deeper into the biofilm to reduce the light intensity or into a less sulfidic layer can, however, prevent the inhibition. Therefore, cyanobacteria like *Planktothrix* str. FS34 are probably effective competitors to obligate anoxygenic phototrophs and to cyanobacteria that can perform both anoxygenic and oxygenic photosynthesis.

Implications for current models of ancient ocean chemistry

The regulatory functions of H_2S on oxygenic photosynthesis identified in this study for the cyanobacterium *Planktothrix* str. FS34 might have played a globally important role before the complete oxygenation of Earth's atmosphere and oceans (Johnston *et al*., 2009) and eventually also during the subsequent sulfidic events that are thought to have caused global mass extinctions [e.g. in the end of Permian period, (Wang, 2012)]. However, it is important to stress in this context that H_2S is advantageous for photosynthesis in cyanobacteria like *Planktothrix* str. FS34 only if the exposure time to H_2S is limited, or if the light intensity or H_2S concentration is low. This means that such cyanobacteria will be competitive as free-living planktonic organisms in a sulfidic water column where H_2S concentrations are not substantially fluctuating only if both light intensity and H_2S concentration are low. The latter implies electron donor limitation for obligate anoxygenic phototrophs. Thus, oxygenic phototrophs like *Planktothrix* str. FS34, which are never limited in electron donor, might have had a selective advantage. Such cyanobacteria would also be successful in environments where H_2S concentrations were fluctuating – either by their own activity (i.e. through the modification of pH) or by the interaction with phototrophic or chemotrophic sulfide oxidizers. In microbial mats that have dominated shallow coastal regions for billions of years and in aggregates formed in the water column, the regulatory functions of H_2S might have provided cyanobacteria like *Planktothrix* str. FS34 a selective advantage. The competitiveness of such obligate oxygenic phototrophs with anoxygenic phototrophs (both obligate and versatile cyanobacteria) in a sulfidic environment was plausibly crucial in the oxygenation process of our planet. This is because the competitiveness implies that oxygenic photosynthesis might have dominated under certain conditions despite abundant electron donor (H_2S) for anoxygenic photosynthesis. The introduction of O_2 to a sulfidic environment would have opened the stage for other competitors to anoxygenic photosynthesis, namely the light-independent aerobic sulfide oxidizers. Therefore, even if their habitat was limited to temporarily fluctuating environments, sulfide-adapted cyanobacteria like *Planktothrix* str. FS34 might have shifted the global balance between anoxygenic and oxygenic photosynthesis, which represents a key aspect of the oxygenation of Earth.

Experimental procedures

Isolation and cultivation

The cyanobacterial strain FS34 was isolated from a biofilm growing in a sulfidic spring emerging from the Frasassi Cave system (Galdenzi *et al*., 2008). Specifically, the culture was obtained by dilution series in sulfidic and non-sulfidic medium and by picking of individual filaments from solid medium as previously described (Klatt *et al*., 2015). The mono-algal culture was not axenic; however, microscopy revealed that the ratio between the cyanobacterial and other cells was > 250. The contaminant cells were most likely not aerobic sulfide oxidizers, as we did not observe any biological sulfide consumption even in the presence of high O_2 concentrations (Fig. 1; Fig. S3). Also their contribution to O_2 removal was < 2%, and therefore negligible (data not shown). During the whole isolation procedure, the cultures were incubated at 15 °C under irradiance of 200 μmol photons m^{-2} s^{-1} provided by fluorescent lamps (Envirolight, USA). For maintenance, cultures were transferred every 3 to 6 weeks alternating to BG–11 and sulfidic Pfennig's medium I.

For the batch reactor experiments, strain FS34 was grown in stirred liquid BG-11 medium until the exponential phase and then transferred into the reactor as previously described (Klatt *et al*., 2015). For the experiments in the flow cell, strain FS34 was also grown in BG-11 medium on a rotary shaker, which led to the formation of floating rigid biofilms that were transferred to and fixed in the flow cell.

Deoxyribonucleic acid extraction, polymerase chain reaction, sequencing and phylogenetic analysis

Deoxyribonucleic acid was extracted as previously described (Ionescu *et al*., 2010; Klatt *et al*., 2015). The partial 16S rRNA gene sequence was amplified using the cyanobacteria-specific primers CYA106F and CYA781R and the parameters for the polymerase chain reaction (PCR) as described by (Nübel *et al*., 1997). The PCR product of the partial 16SrRNA sequence was purified using the QIAquick PCR purification kit (Qiagen) and Sanger sequenced as previously described (Klatt *et al*., 2015). The partial 16S rRNA gene sequence is deposited in the European Nucleotide Archive under the accession number LN609763.

For phylogenetic analysis, the 16S rRNA sequence was aligned with SINA (Pruesse *et al*., 2012), and was merged with the SILVA SSURef_NR99_115 dataset (Quast *et al*., 2013) for further processing using software package ARB (Ludwig *et al*., 2004). Along with the strain FS34 16S rRNA gene sequence, 20 full-length 16S rRNA gene sequences from other cultivated strains belonging to the *Oscillatoriales* order were selected for phylogenetic tree reconstruction. Several treeing algorithms (neighbour joining, maximum parsimony and maximum likelihood) with and without

alignment position and base conservation filters were applied, and each attempt returned almost identical tree topologies. The final tree shown is calculated using RAxML version 7.0.4, with a GTRGAMMA model, a 10% cyanobacterial base conservation filter, and with 1000 bootstraps. The FS34 sequence was added later to this tree using the ARB parsimony insertion tool, again applying the 10% base conservation filter.

Stirred batch reactor experiment

To test whether strain FS34 is capable of anoxygenic photosynthesis using sulfide as an electron donor, culture harvested in the exponential growth phase was incubated in a stirred batch reactor without headspace (Klatt *et al*., 2015). The set-up allows online measurement of O_2 concentration and pH and the assessment of the S_{tot} concentrations in subsamples taken during an incubation. In this experiment, we exposed the culture to S_{tot} concentrations of up to 400 μM ($[H_2S] = 60$ μM) for 5 min–20 h in the dark, switched on the light (irradiance 20–500 μmol photons m^{-2} s^{-1}) and measured O_2 production and S_{tot} consumption rates for at least 6 h.

Flow-through chamber with a sulfidic bottom reservoir

The experimental set-up used for the measurements of photosynthesis in the biofilms formed by the studied cyanobacterial strain consisted of a top part that was constructed like a flow-through chamber (height: 10 cm, length: 25 cm, depth: 10 cm) and placed on top of a stirred reservoir (volume 2.4 L) (Fig. S1). The reservoir was filled with BG-11 medium to which Na_2S stock solution (pH ~7.5, 200 mM) could be added by injection through a butyl rubber stopper. The chamber was separated from the reservoir by a polyester fibrous web on which the biofilm was fixed with pins. The flow chamber was fed from a thermostated recycle via gas-tight tubing. O_2 concentration in the recycle and consequentially in the water column was adjusted by bubbling with nitrogen gas. To reduce exchange with air, paraffin oil was added on the water surface of the flow chamber, and the thermostated recycle was covered with foil. Sulfide gradients across the biofilms were generated by the addition of sodium sulfide from a stock solution to the reservoir and in some cases also to the recycle.

Illumination of the biofilms in the flow chamber was provided by a halogen lamp (Schott KL2500). The incident irradiance at the surface of the biofilm was determined with a submerged cosine-corrected quantum sensor connected to a LI-250A light meter (both LI-COR Biosciences GmbH, Germany).

Microsensors

O_2, pH and H_2S microsensors with a tip diameter of 10–30 μm and response time of < 1 s were built, calibrated and used as previously described (Revsbech, 1989; Jeroschewski *et al*., 1996; de Beer *et al*., 1997). Calibration of the H_2S microsensors was performed in an acidified BG-11 medium (pH < 2) to which Na_2S was added stepwise. The S_{tot} concentrations in the calibration solution were determined according to Cline (1969).

Microsensor measurements

During simultaneous O_2, pH and H_2S measurements, the tips of the microsensors were always separated by less than 50 μm. Depth profiles were corrected for the azimuthal angle at which they were measured (Berg *et al*., 1998; Polerecky *et al*., 2007). Calculation of S_{tot} from the local H_2S concentrations and pH values measured with microsensors was done according to Millero (1986), using a pK value of 7.14 (Wieland and Kühl, 2000). Volumetric rates of GP were determined using the O_2 microsensor based light-dark shift method (Revsbech and Jørgensen, 1983).

Acknowledgements

We thank Georg Herz and Jürgen Kohl from the mechanical workshop for their help with the construction of the experimental setup, the technicians of the microsensor group for the construction of microsensors, J. Macalady and D. S. Jones for their support during field campaigns, A. Montanari and P. Metallo for their hospitality during the sampling campaign at the Osservatorio Geologico di Coldigioco and S. Meyer for her support during isolation and cultivation. This work was financially supported by the Max Planck Society.

Conflicts of interest

The authors declare no conflicts of interest.

References

Allen, J.F., Mullineaux, C.W., Sanders, C.E., and Melis, A. (1989) State transitions, photosystem stoichiometry adjustment and non-photochemical quenching in cyanobacterial cells acclimated to light absorbed by photosystem I or photosystem II. *Photosynth Res* **22:** 157–166.

Beauchamp, R.O., Bus, J.S., Popp, J.A., Boreiko, C.J., and Andjelkovich, D.A. (1984) A critical review of the literature on hydrogen sulfide toxicity. *Crit Rev Toxicol* **13:** 25–97.

de Beer, D., Schramm, A., Santegoeds, C.M., and Kühl, M. (1997) A nitrite microsensor for profiling environmental biofilms. *Appl Environ Microbiol* **63:** 973–977.

Berg, P., Risgaard-Petersen, N., and Rysgaard, S. (1998) Interpretation of measured concentration profiles in sediment pore water. *Limnol Oceanogr* **43:** 1500–1510.

Bloem, E., Riemenschneider, A., Volker, J., Papenbrock, J., Schmidt, A., Salac, I., *et al*. (2004) Sulphur supply and infection with *Pyrenopeziza brassicae* influence L-cysteine desulphydrase activity in *Brassica napus* L. *J Exp Bot* **55:** 2305–2312.

Buchanan, B.B. (1991) Regulation of CO2 assimilation in oxygenic photosynthesis: the ferredoxin/thioredoxin system. *Arch Biochem Biophys* **288:** 1–9.

Buick, R. (2008) When did oxygenic photosynthesis evolve? *Philos Trans R Soc Lond B Biol Sci* **363:** 2731–2743.

Canfield, D.E. (1998) A new model for Proterozoic ocean chemistry. *Nature* **396:** 450–453.

Cardol, P., Forti, G., and Finazzi, G. (2011) Regulation of electron transport in microalgae. *Biochim Biophys Acta* **1807:** 912–918.

Chen, J., Wu, F.-H., Wang, W.-H., Zheng, C.-J., Lin, G.-H., Dong, X.-J., *et al*. (2011) Hydrogen sulphide enhances photosynthesis through promoting chloroplast biogenesis, photosynthetic enzyme expression, and thiol redox modification in *Spinacia oleracea* seedlings. *J Exp Bot* **62:** 4481–4493.

Cline, J.D. (1969) Oxygenation of hydrogen sulfide in seawater at constant salinity, temperature and pH. *Environ Sci Technol* **3:** 838–843.

Cohen, Y., Jørgensen, B.B., Padan, E., and Shilo, M. (1975) Sulphide-dependent anoxygenic photosynthesis in the cyanobacterium *Oscillatoria limnetica*. *Nature* **257:** 489–492.

Cohen, Y., Jørgensen, B.B., Revsbech, N.P., and Poplawski, R. (1986) Adaptation to hydrogen sulfide of oxygenic and anoxygenic photosynthesis among Cyanobacteria. *Appl Environ Microbiol* **51:** 398–407.

Cooper, C.E., and Brown, G.C. (2008) The inhibition of mitochondrial cytochrome oxidase by the gases carbon monoxide, nitric oxide, hydrogen cyanide and hydrogen sulfide: chemical mechanism and physiological significance. *J Bioenerg Biomembr* **40:** 533–539.

Dooley, F.D., Wyllie-Echeverria, S., Roth, M.B., and Ward, P.D. (2013) Tolerance and response of Zostera marina seedlings to hydrogen sulfide. *Aquat Bot* **105:** 7–10.

Dorman, D.C. (2002) Cytochrome oxidase inhibition induced by acute hydrogen sulfide inhalation: correlation with tissue sulfide concentrations in the rat brain, liver, lung, and nasal epithelium. *Toxicol Sci* **65:** 18–25.

Eilers, P.H.C., and Peeters, J.C.H. (1988) A model for the relationship between light intensity and the rate of photosynthesis in phytoplankton. *Ecol Modell* **42:** 199–215.

Galdenzi, S., Cocchioni, M., Morichetti, L., Amici, V., and Scuri, S. (2008) Sulfidic ground-water chemistry in the Frasassi caves, Italy. *J Caves Karst Stud* **70:** 94–107.

García-Mata, C., and Lamattina, L. (2010) Hydrogen sulphide, a novel gasotransmitter involved in guard cell signalling. *New Phytol* **188:** 977–984.

Garcia-Pichel, F., and Castenholz, R.W. (1990) Comparative anoxygenic photosynthetic capacity in 7 strains of a thermophilic cyanobacterium. *Arch Microbiol* **153:** 344–351.

Ghysels, B., Godaux, D., Matagne, R.F., Cardol, P., and Franck, F. (2013) Function of the chloroplast hydrogenase in the microalga Chlamydomonas: the role of hydrogenase and state transitions during photosynthetic activation in anaerobiosis. *PLoS ONE* **8:** e64161.

Hancock, J.T., Lisjak, M., Teklic, T., Wilson, I.D., and Whiteman, M. (2011) Hydrogen sulfide and signaling in plants. In *Plant Sciences Reviews*. Hemming, D. (ed.). Oxfordshire, UK: CABI, pp. 33–40.

Ionescu, D., Voss, B., Oren, A., Hess, W.R., and Muro-Pastor, A.M. (2010) Heterocyst-specific transcription of NsiR1, a non-coding RNA encoded in a tandem array of direct repeats in cyanobacteria. *J Mol Biol* **398:** 177–188.

Jablonsky, J., and Lazar, D. (2008) Evidence for intermediate S-states as initial phase in the process of oxygen-evolving complex oxidation. *Biophys J* **94:** 2725–2736.

Jeroschewski, P., Steuckart, C., and Kühl, M. (1996) An amperometric microsensor for the determination of H2S in aquatic environments. *Anal Chem* **68:** 4351–4357.

Jin, Z., Shen, J., Qiao, Z., Yang, G., Wang, R., and Pei, Y. (2011) Hydrogen sulfide improves drought resistance in *Arabidopsis thaliana*. *Biochem Biophys Res Commun* **414:** 481–486.

Johnston, D.T., Wolfe-Simon, F., Pearson, A., and Knoll, A.H. (2009) Anoxygenic photosynthesis modulated Proterozoic oxygen and sustained Earth's middle age. *Proc Natl Acad Sci USA* **106:** 16925–16929.

Jørgensen, B.B., Cohen, Y., and Revsbech, N.P. (1986) Transition from anoxygenic to oxygenic photosynthesis in a microcoleus chthonoplastes Cyanobacterial mat. *Appl Environ Microbiol* **51:** 408–417.

Klatt, J.M., Al-Najjar, M.A.A., Yilmaz, P., Lavik, G., de Beer, D., and Polerecky, L. (2015) Anoxygenic photosynthesis controls oxygenic photosynthesis in a cyanobacterium from a sulfidic spring. *Appl Environ Microbiol* AEM.03579–14. DOI:10.1128/AEM.03579-14.

Lamers, L.P.M., Govers, L.L., Janssen, I.C.J.M., Geurts, J.J.M., Van der Welle, M.E.W., Van Katwijk, M.M., *et al*. (2013) Sulfide as a soil phytotoxin-a review. *Front Plant Sci* **4:** 268.

Li, Z.-G., Gong, M., Xie, H., Yang, L., and Li, J. (2012) Hydrogen sulfide donor sodium hydrosulfide-induced heat tolerance in tobacco (*Nicotiana tabacum* L) suspension cultured cells and involvement of Ca(2+) and calmodulin. *Plant Sci* **185–186:** 185–189.

Lisjak, M., Srivastava, N., Teklic, T., Civale, L., Lewandowski, K., Wilson, I., *et al*. (2010) A novel hydrogen sulfide donor causes stomatal opening and reduces nitric oxide accumulation. *Plant Physiol Biochem* **48:** 931–935.

Lisjak, M., Teklic, T., Wilson, I.D., Whiteman, M., and Hancock, J.T. (2013) Hydrogen sulfide: environmental factor or signalling molecule? *Plant Cell Environ* **36:** 1607–1616.

Ludwig, W., Strunk, O., Westram, R., Richter, L., Meier, H., Yadhukumar, *et al*. (2004) ARB: a software environment for sequence data. *Nucleic Acids Res* **32:** 1363–1371.

McDonald, A.E., Ivanov, A.G., Bode, R., Maxwell, D.P., Rodermel, S.R., and Hüner, N.P.A. (2011) Flexibility in photosynthetic electron transport: the physiological role of plastoquinol terminal oxidase (PTOX). *Biochim Biophys Acta* **1807:** 954–967.

McFadden, G.I. (2001) Primary and secondary endosymbiosis and the origin of plastids. *J Phycol* **37:** 951–959.

Michelet, L., Zaffagnini, M., Morisse, S., Sparla, F., Pérez-Pérez, M.E., Francia, F., *et al*. (2013) Redox regulation of the Calvin–Benson cycle: something old, something new. *Front Plant Sci* **4:** 470.

Miller, S.R., and Bebout, B.M. (2004) Variation in sulfide tolerance of photosystem II in phylogenetically diverse cyanobacteria from sulfidic habitats. *Appl Environ Microbiol* **70:** 736–744.

Millero, F. (1986) The thermodynamics and kinetics of the hydrogen sulfide system in natural waters. *Mar Chem* **18:** 121–147.

Mulkidjanian, A.Y., Koonin, E.V., Makarova, K.S., Mekhedov, S.L., Sorokin, A., Wolf, Y.I., *et al*. (2006) The

cyanobacterial genome core and the origin of photosynthesis. *Proc Natl Acad Sci USA* **103:** 13126–13131.
Nisbet, E.G., and Fowler, C.M.R. (1999) Archaean metabolic evolution of microbial mats. *Proc Biol Sci* **266:** 2375–2382.
Nübel, U., Garcia-Pichel, F., and Muyzer, G. (1997) PCR primers to amplify 16S rRNA genes from cyanobacteria. *Appl Environ Microbiol* **63:** 3327–3332.
Polerecky, L., Bachar, A., Schoon, R., Grinstein, M., Jørgensen, B.B., de Beer, D., and Jonkers, H.M. (2007) Contribution of Chloroflexus respiration to oxygen cycling in a hypersaline microbial mat from Lake Chiprana, Spain. *Environ Microbiol* **9:** 2007–2024.
Pruesse, E., Peplies, J., and Glöckner, F.O. (2012) SINA: accurate high-throughput multiple sequence alignment of ribosomal RNA genes. *Bioinformatics* **28:** 1823–1829.
Quast, C., Pruesse, E., Yilmaz, P., Gerken, J., Schweer, T., Yarza, P., *et al*. (2013) The SILVA ribosomal RNA gene database project: improved data processing and web-based tools. *Nucleic Acids Res* **41:** D590–D596.
Rausch, T., and Wachter, A. (2005) Sulfur metabolism: a versatile platform for launching defence operations. *Trends Plant Sci* **10:** 503–509.
Rennenberg, H., and Filner, P. (1983) Developmental changes in the potential for H2S emission in cucurbit plants. *Plant Physiol* **71:** 269–275.
Revsbech, N.P. (1989) An oxygen microsensor with a guard cathode. *Limnol Oceanogr* **34:** 474–478.
Revsbech, N.P., and Jørgensen, B.B. (1983) Photosynthesis of benthic microflora measured with high spatial resolution by the oxygen microprofile method: capabilities and limitations of the method. *Limnol Oceanogr* **28:** 749–759.
Revsbech, N.P., Jørgensen, B.B., Blackburn, T.H., and Cohen, Y. (1983) Microelectrode studies of the photosynthesis and O2, H2S and pH profiles of a microbial mat. *Limnol Oceanogr* **28:** 1062–1074.
Schreiber, U., Gademann, R., Bird, P., Ralph, P.J., Larkum, A.W.D., and Kuhl, M. (2002) Apparent light requirement for activation of photosynthesis upon rehydration of desiccated beachrock microbial mats. *J Phycol* **38:** 125–134.
Schürmann, P., and Buchanan, B.B. (2008) The ferredoxin/thioredoxin system of oxygenic photosynthesis. *Antioxid Redox Signal* **10:** 1235–1274.
Seckbach, J., and Oren, A. (2010) *Microbial Mats: Modern and Ancient Microorganisms in Stratified Systems*. Dordrecht: Springer.
Shen, J., Xing, T., Yuan, H., Liu, Z., Jin, Z., Zhang, L., and Pei, Y. (2013) Hydrogen sulfide improves drought tolerance in Arabidopsis thaliana by microRNA expressions. *PLoS ONE* **8:** e77047.
Soetaert, K.E.R., Petzoldt, T., and Setzer, R.W. (2010) Solving differential equations in R: package deSolve. *J Stat Softw* **33:** 1–25.
Stuiver, C.E.E., De Kok, L.J., and Kuiper, P.J.C. (1992) Freezing tolerance and biochemical changes in wheat shoots as affected by H2S fumigation. *Plant Physiol Biochem* **30:** 47–55.
Sukenik, A., Bennett, J., and Falkowski, P. (1987) Light-saturated photosynthesis – limitation by electron transport or carbon fixation? *Biochim Biophys Acta* **891:** 205–215.
Voorhies, A.A., Biddanda, B.A., Kendall, S.T., Jain, S., Marcus, D.N., Nold, S.C., *et al*. (2012) Cyanobacterial life at low O(2): community genomics and function reveal metabolic versatility and extremely low diversity in a Great Lakes sinkhole mat. *Geobiology* **10:** 250–267.
Wang, R. (2012) Physiological implications of hydrogen sulfide: a whiff exploration that blossomed. *Physiol Rev* **92:** 791–896.
Wieland, A., and Kühl, M. (2000) Short-term temperature effects on oxygen and sulfide cycling in a hypersaline cyanobacterial mat (Solar Lake, Egypt). *Mar Ecol Prog Ser* **196:** 87–102.
Zhang, H., Hu, L.-Y., Hu, K.-D., He, Y.-D., Wang, S.-H., and Luo, J.-P. (2008) Hydrogen sulfide promotes wheat seed germination and alleviates oxidative damage against copper stress. *J Integr Plant Biol* **50:** 1518–1529.
Zhang, H., Ye, Y.-K., Wang, S.-H., Luo, J.-P., Tang, J., and Ma, D.-F. (2009) Hydrogen sulfide counteracts chlorophyll loss in sweetpotato seedling leaves and alleviates oxidative damage against osmotic stress. *Plant Growth Regul* **58:** 243–250.
Zhang, H., Hu, L.-Y., Li, P., Hu, K.-D., Jiang, C.-X., and Luo, J.-P. (2010) Hydrogen sulfide alleviated chromium toxicity in wheat. *Biol Plant* **54:** 743–747.

Supporting information

Additional Supporting Information may be found in the online version of this article at the publisher's web-site:

Fig. S1. Schematic diagram of the flow-through chamber used in this study. Biofilms (a) were fixed on a polyester fibrous web (b) that separated the flowing water column of the upper part from the reservoir in the bottom part. Sodium sulfide stock solution was added to the reservoir through a butyl rubber stopper (c). Mixing in the bottom part was achieved by a magnetic glass stir bar (d).
Fig. S2. Light microscope image of *Planktothrix* str. FS34 (scale bar is 5 μm) and a dendrogram showing the position of its 16S rRNA sequence with respect to sequences from other cultivated members of *Oscillatoriales*. The tree reconstruction was performed using maximum likelihood algorithm as implemented in RAxML. The two *Gloeobacter violaceus* sequences serve as the out-group. Bootstrap values are only shown when they were above 60%; the bar indicates 0.02 substitutions per nucleotide position.
Fig. S3. Oxygen and total sulfide concentration dynamics measured in a stirred batch reactor filled with *Planktothrix* str. FS34 culture. Sodium sulfide stock solution was added to the culture in the dark to establish a final S_{tot} concentration of 400 μM ($[H_2S] = 95$ μM) in the reactor. Scalar irradiance in the reactor was 100 μmol photons m^{-2} s^{-1}. The decrease in the S_{tot} concentration in the presence of photosynthetically produced oxygen was due to abiotic sulfide oxidation as confirmed by separate incubations of medium without culture.